



### TRANSPLANTATION

# Ruxolitinib protects skin stem cells and maintains skin homeostasis in murine graft-versus-host disease

Shuichiro Takahashi,<sup>1</sup> Daigo Hashimoto,<sup>1</sup> Eiko Hayase,<sup>1</sup> Reiki Ogasawara,<sup>1</sup> Hiroyuki Ohigashi,<sup>1</sup> Takahide Ara,<sup>1</sup> Emi Yokoyama,<sup>1</sup> Ko Ebata,<sup>1</sup> Satomi Matsuoka,<sup>1</sup> Geoffrey R. Hill,<sup>2</sup> Junichi Sugita,<sup>1</sup> Masahiro Onozawa,<sup>1</sup> and Takanori Teshima<sup>1</sup>

<sup>1</sup>Department of Hematology, Faculty of Medicine, Hokkaido University, Sapporo, Japan; and <sup>2</sup>Department of Immunology, QIMR Berghofer Medical Research Institute, Brisbane, QLD, Australia

#### KEY POINTS

- Skin GVHD targets Lgr5<sup>+</sup> HFSCs in association with impaired hair regeneration and wound healing.
- Topical ruxolitinib, unlike corticosteroids, protects Lgr5<sup>+</sup> skin stem cells and maintains skin homeostasis in skin GVHD.

**Graft-versus-host disease (GVHD) is the major complication after allogeneic stem cell transplantation (SCT). Emerging evidence indicates that GVHD leads to injury of intestinal stem cells. However, it remains to be investigated whether skin stem cells could be targeted in skin GVHD. Lgr5<sup>+</sup> hair follicle stem cells (HFSCs) contribute to folliculogenesis and have a multipotent capacity to regenerate all epithelial cells in repair. We studied the fate of Lgr5<sup>+</sup> HFSCs after SCT and explored the novel treatment to protect Lgr5<sup>+</sup> HFSCs against GVHD using murine models of SCT. We found that GVHD reduced Lgr5<sup>+</sup> HFSCs in association with impaired hair regeneration and wound healing in the skin after SCT. Topical corticosteroids, a standard of care for a wide range of skin disorders including GVHD, damaged HFSCs and failed to improve skin homeostasis, despite of their anti-inflammatory effects. In contrast, JAK1/2 inhibitor ruxolitinib significantly ameliorated skin GVHD, protected Lgr5<sup>+</sup> HFSCs, and restored hair regeneration and wound healing after SCT. We, for the first time, found that GVHD targets Lgr5<sup>+</sup> HFSCs and that topical ruxolitinib represents a novel strategy to protect skin stem cells and maintain skin homeostasis in GVHD. (*Blood*. 2018;131(18):2074-2085)**

## Introduction

Allogeneic hematopoietic stem cell transplantation (SCT) is a curative therapy for hematologic malignancies and bone marrow failure syndrome. Graft-versus-host disease (GVHD) remains a major obstacle to performing SCT. Adult tissue stem cells have emerged as targets of GVHD. Intestinal GVHD leads to loss of Lgr5<sup>+</sup> intestinal stem cells (ISCs).<sup>1,2</sup> ISC injury is associated with profound damage of intestinal epithelium, impairing physiological repair and causing refractory colitis in GVHD. Thus, protection of ISCs will pave a new avenue to improving the outcome of allogeneic SCT.<sup>1-3</sup>

The skin is the most frequently involved tissue in both acute and chronic GVHD. Particularly, 15% of acute GVHD solely involves skin without other organ manifestations.<sup>4</sup> The skin is highly dynamic tissue harboring several distinct populations of stem cells to maintain homeostasis. In mice, the epidermis is maintained in discrete compartments during homeostasis. Hair follicle stem cells (HFSCs) reside in the hair follicle bulge; hair germ maintain lower hair follicles, whereas Lrig1<sup>+</sup> stem cells in isthmus maintain the upper pilosebaceous units in steady state.<sup>5</sup> However, both populations acquire lineage plasticity and make a contribution to regenerative skin upon wounding.<sup>5</sup> HFSCs are the best-characterized stem cell population in the hair bulge

because of their expression of a set of distinct markers, such as cytokeratin-15 (CK15) and CD34.<sup>6,7</sup> Subsequent studies have further specified the phenotypes and functions of HFSCs, demonstrating that HFSCs with multipotent plasticity are enriched in the Lgr5<sup>+</sup> cell fraction among them.<sup>5,8</sup>

Repair of severe skin injury requires skin regeneration from skin stem cells. Therefore, damage of skin stem cells is associated with prolonged skin injury and impaired skin homeostasis. A series of previous experimental and clinical studies of skin GVHD have shown that apoptotic cells accompanying donor T-cell infiltration are spatially restricted to the sites harboring stem-cell populations such as bulge regions of hair follicles, human epidermal rete ridges, and the rete-like prominences (RLPs) of murine tongue, as a surrogate of human rete ridges.<sup>9-15</sup> Although previous studies demonstrated injury of CK15<sup>+</sup> stem cells in RLPs of the murine tongue during GVHD,<sup>11,12</sup> it remains to be elucidated whether, using modern sophisticated model systems, Lgr5<sup>+</sup> HFSCs could be targets of GVHD and the dynamic process of damage and repopulation of HFSCs, which play a pivotal role in the competitive race between tissue damage and restoration during GVHD needs to be clarified.

Topical corticosteroids are the standard of care for a wide range of skin disorders such as GVHD. However, besides their

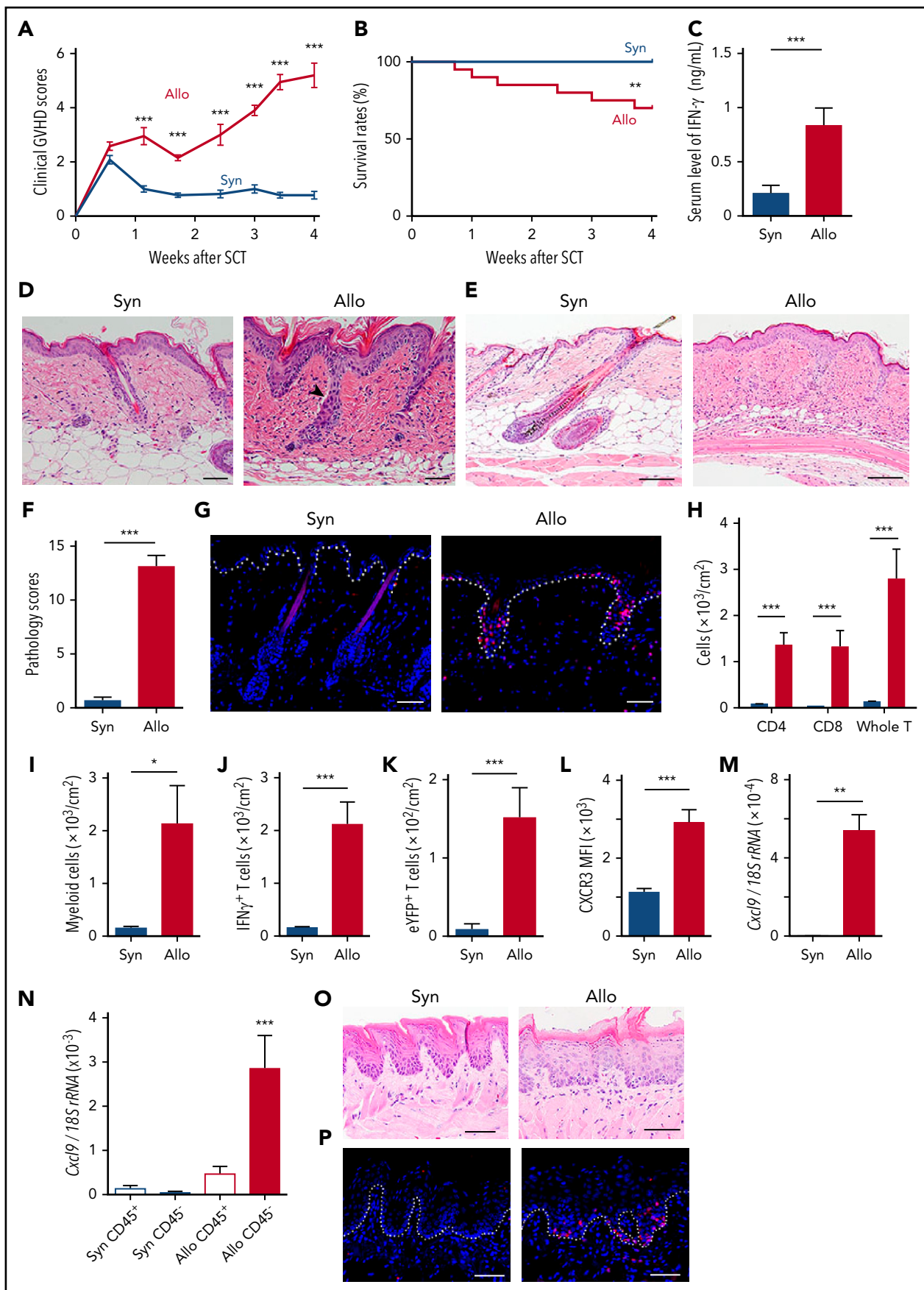


Figure 1.

anti-inflammatory actions, long-term use of corticosteroids induces adverse effects on skin such as skin atrophy and delayed wound healing.<sup>16</sup> Mechanisms of such adverse effects are not well understood. In this study, we addressed these issues using *Lgr5* reporter mice and explored a novel strategy to protect *Lgr5*<sup>+</sup> HFSCs to ameliorate skin GVHD with topical administration of JAK1/2 inhibitor ruxolitinib.

## Methods

### Mice

The mouse strains used are described in the supplemental Methods (available on the *Blood* Web site).

### SCT

Mice were transplanted as previously described.<sup>17</sup> Briefly, recombinant human granulocyte colony-stimulating factor (G-CSF; Kyowa Hakko Kirin Co Ltd, Tokyo, Japan) was administered subcutaneously to donor mice at 10  $\mu$ g daily from day  $-6$  to day  $-1$ . Mice at 8- to 10-weeks-old received 10.5 Gy total-body irradiation (TBI), split into 2 doses with a 4-hour interval, on day  $-1$ , followed by IV injection of  $20 \times 10^6$  splenocytes from G-CSF-treated syngeneic or allogeneic donors on day 0. Transplanted mice were kept in a specific pathogen-free condition with normal chow and autoclaved hyperchlorinated water. Survival of recipient mice was monitored daily and clinical GVHD scores, incorporating 5 clinical parameters such as weight loss, posture, activity, fur texture, and skin integrity, were assessed weekly as previously described.<sup>18</sup> Fur texture and skin integrity were assessed in the depilated skin, where no topical treatment was administered.

### Reagents

Ruxolitinib ointment 0.5% was formulated by mixing ruxolitinib phosphate salt (LC Laboratories, Woburn, MA) dissolved in dimethyl sulfoxide with Vaseline. Vaseline with dimethyl sulfoxide was used as a control ointment. For systemic administration, ruxolitinib was dissolved in ethanol and diluted with phosphate-buffered saline with 0.1% Tween 20, and orally administered at a dose of 30 mg/kg to the recipient mice twice daily from day  $+1$  after SCT. Prednisolone sodium succinate (Shionogi, Osaka, Japan) in phosphate-buffered saline was orally administered at a dose of 10 mg/kg to the recipient mice once daily from day  $+1$  after SCT. Betamethasone valerate and clobetasol propionate were obtained from Shionogi and Sigma-Aldrich (St. Louis, MO), respectively.

### Cell isolation and flow cytometry

The detailed protocols are described in the supplemental Methods.

### Skin incisional wounding

After anesthetization, a full-thickness round skin was removed from the shaved back of C57BL/6, *B6-Lgr5<sup>EGFP-cre/ER</sup> × R26<sup>tdTomato</sup>* mice using a 5-mm disposable punch biopsy instrument (DermaPunch; Nipro, Osaka, Japan). The wound was digitally photographed, and the scale and area of skin wounds were assessed with NIH ImageJ software (<https://imagej.nih.gov/ij/>). For the fate mapping of *Lgr5*<sup>+</sup> cells, 1 mg of tamoxifen was orally given to *B6-Lgr5<sup>EGFP-cre/ER</sup> × R26<sup>tdTomato</sup>* mice for 6 days before wounding.

### Histology and immunofluorescent study

The detailed protocols are described in the supplemental Methods.

### Q-PCR

Total RNA from back skin was extracted using ISOGEN II (Nippon Gene, Tokyo, Japan). Reverse transcription was conducted with ReverTra Ace qPCR RT Master Mix with gDNA Remover (Toyobo Life Science, Osaka, Japan). Quantitative real-time polymerase chain reaction (Q-PCR) was performed with specific primer and probe sets (Sigma-Aldrich; the sequences are listed in supplemental Table 2) and TaqMan Fast Advanced Master Mix (Thermo Fisher Scientific, Waltham, MA) on the StepOnePlus real-time PCR system (Thermo Fisher Scientific). All measurements were normalized against the expression of the internal control 18S ribosomal RNA. Relative amounts of each messenger RNA were calculated by the comparative  $\Delta$  cycle threshold method.

### Statistics

The Mann-Whitney *U* test or 1-way analysis of variance (ANOVA) followed by the Tukey posttest was used to compare the data. The Kaplan-Meier product limit method was used to obtain survival probability and the log-rank test was used for the comparison between survival curves.  $P < .05$  was considered statistically significant, and all data represent the mean  $\pm$  standard error of the mean (SEM). All tests were performed using the program GraphPad Prism 6 (La Jolla, CA).

## Results

### Hair follicles in the skin and rete-like prominences in the lingual epithelium are targets for GVHD

First, we evaluated whether GVHD could damage the hair follicles and RLPs, where skin stem cells reside in well-established mouse models of skin GVHD, in which transition from acute to chronic GVHD in the skin could be observed.<sup>17</sup> *B6* mice were lethally irradiated with 10.5 Gy TBI on day  $-1$  and IV injected with  $20 \times 10^6$  splenocytes from G-CSF-treated allogeneic BALB/c or syngeneic *B6* donors on day 0. Morbidity and mortality of

**Figure 1. Hair follicles and rete-like prominences in the lingual epithelium are damaged in GVHD.** Lethally irradiated *B6* mice were transplanted with  $20 \times 10^6$  G-CSF-mobilized splenocytes from syngeneic (Syn) *B6* or allogeneic (Allo) BALB/c mice on day 0, except for (G,P) using *B6-Lck-Cre × R26<sup>tdTomato</sup>* and for (K) using *B6-Il17a<sup>Cre</sup> × R26<sup>eYFP</sup>* as donors. (A) Clinical GVHD scores from 3 experiments ( $n = 11$  per group). (B) Survival curves from 6 independent experiments ( $n = 20$  per group). (C) Serum levels of IFN- $\gamma$  on day  $+14$  after SCT from 3 independent experiments ( $n = 8-10$  per group). (D-F) The back skins were harvested on day  $+14$  (D) and  $+28$  (E-F) after SCT. The representative images of hematoxylin and eosin (H&E) staining (D-E) and pathological GVHD scores (F) from 3 independent experiments. The arrowhead indicates dermal epidermal detachment. (G) Immunofluorescent images of *tdTomato*<sup>+</sup> donor T cells (red) with 4',6-diamidino-2-phenylindole (DAPI) nuclear staining (blue) in the skin harvested on day  $+10$  after SCT. Dashed line shows the epidermal-dermal junction. (H-L) Flow cytometric analysis of skin-infiltrating cells on day  $+14$  after SCT. The absolute numbers of donor T cells (H), CD11b<sup>+</sup> myeloid cells (I), IFN- $\gamma$ <sup>+</sup> T cells (J), IL-17eYFP<sup>+</sup> T cells (K), and mean fluorescence intensity (MFI) of CXCR3 on T cells (L) from 2 experiments ( $n = 8-10$  per group). (M-N) Total RNA was extracted from the whole skin (M) or purified CD45<sup>+</sup> cells and CD45<sup>-</sup> cells from the back skin (N) on day  $+14$  after SCT and the expression of *Cxcl9* was evaluated by Q-PCR ( $n = 8-10$  per group from 2 independent experiments). H&E staining (O) and immunofluorescent staining of *tdTomato*<sup>+</sup> donor T cells (red) with DAPI (blue) staining (P) of lingual samples harvested on day  $+7$  after SCT. Dashed line shows the junction of epithelium and lamina propria. Original magnification  $\times 20$  (D,G,O,P) and  $\times 10$  (E). Scale bar, 50  $\mu$ m. The Mann-Whitney *U* test or 1-way ANOVA followed by the Tukey posttest was used to compare the data (\* $P < .05$ ; \*\* $P < .01$ ; \*\*\* $P < .005$ ). Data represent the mean  $\pm$  SEM. rRNA, ribosomal RNA.

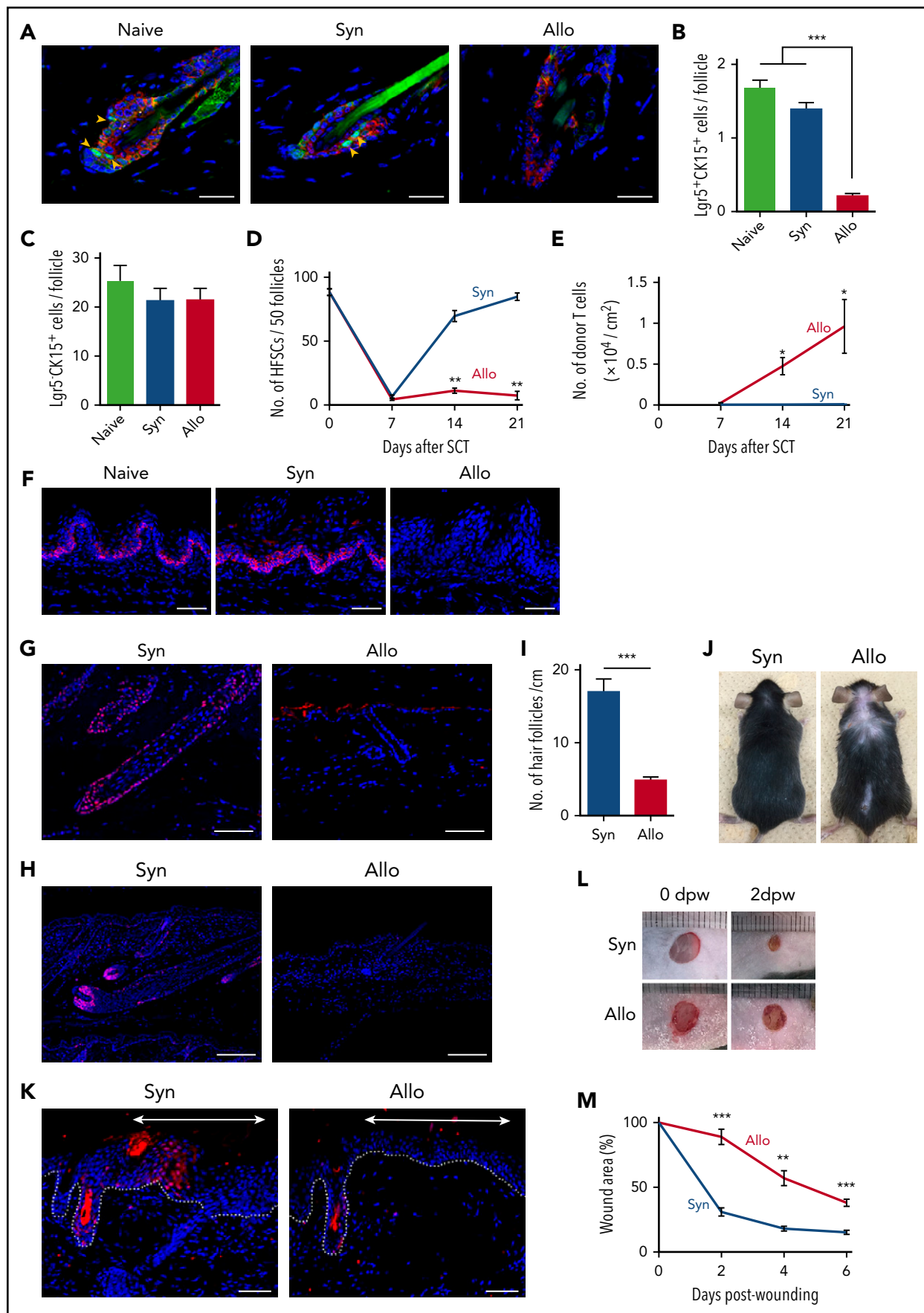


Figure 2.

GVHD were significantly higher after allogeneic SCT than those after syngeneic SCT (Figure 1A-B). Serum levels of IFN- $\gamma$  were significantly elevated after allogeneic SCT (Figure 1C). Skin histology on day +14 showed the acute phase of skin GVHD, such as mononuclear cell infiltration into the epidermal-dermal junction and hair follicles, as well as dermal epidermal detachment (Figure 1D). Subsequent skin histology on day +28 showed standard pathological features of chronic GVHD, including mononuclear cell infiltrates, atrophy of hair follicle and fat layer, and dermal fibrosis (Figure 1E). Skin pathology scores<sup>17</sup> were significantly higher in allogeneic mice than those in syngeneic controls (Figure 1F).

We then focused on the acute phase of skin GVHD. When B6-Lck-cre  $\times$  R26<sup>tdTomato</sup> mice were used as donors to specifically label donor T cells with tdTomato, immunofluorescent studies showed that the epidermal-dermal junction and hair follicles were preferentially infiltrated with donor T cells 10 days after allogeneic SCT (Figure 1G). Flow cytometric analysis of the skin showed significant accumulation of donor T cells and CD11b<sup>+</sup> myeloid cells on day +14 after allogeneic SCT (Figure 1H-I). Intracellular cytokine staining showed skin infiltration of interferon- $\gamma$  (IFN- $\gamma$ )-producing donor T cells after allogeneic SCT (Figure 1J). When interleukin-17A (IL-17A) fate-mapping mice,<sup>19,20</sup> in which IL-17A-producing cells and their progenies were visually labeled, were used as donors, skin infiltration of enhanced yellow fluorescent protein-positive (eYFP<sup>+</sup>) donor T cells was significantly increased in allogeneic mice compared with syngeneic controls (Figure 1K). Donor T-cell CXCR3 plays an important role in T-cell migration to the skin in GVHD.<sup>21</sup> After allogeneic SCT, expression of CXCR3 in skin-infiltrating donor T cells and its ligand *Cxcl9* in the skin was upregulated (Figure 1L-M). We found that *Cxcl9* expression was predominantly upregulated in the CD45<sup>-</sup> cell fraction and, to a much lesser extent, in CD45<sup>+</sup> cells, indicating that CD45<sup>-</sup> nonhematopoietic cells are the major producer of CXCL9 after allogeneic SCT (Figure 1N).

Because mouse skin is devoid of rete ridges, where epidermal stem cells reside in human, we assessed RLPs in the mouse dorsal tongue as the surrogates for human rete ridges.<sup>11,12</sup> Histopathological analysis of RLPs showed evidences of GVHD, including tdTomato<sup>+</sup> donor T-cell infiltration, hyperkeratosis, and blurring of rete-like structures (Figure 1O-P). Altogether, we conclude that this SCT model is appropriated to analyze the fate of skin stem cells and explore the impact of therapeutic intervention on those cells.

### Lgr5<sup>+</sup> HFSC injury is associated with impairment of wound healing and hair regeneration

Next, we examined the fate of Lgr5<sup>+</sup> HFSCs posttransplant in Lgr5 reporter B6-Lgr5<sup>EGFP-cre/ER</sup> mice, in which Lgr5<sup>+</sup> cells were

labeled with enhanced green fluorescent protein (EGFP). Lgr5<sup>+</sup> HFSCs reside in the lower bulge lesion of hair follicles and are CK15<sup>+</sup>. Double-immunofluorescent staining of EGFP and CK15 of the skin harvested 14 days after SCT showed that Lgr5<sup>+</sup> HFSCs residing at lower bulge persisted after syngeneic SCT, but were markedly reduced after allogeneic SCT (Figure 2A). Lgr5<sup>+</sup>CK15<sup>+</sup> cell numbers per follicle were significantly fewer after allogeneic SCT, in contrast to more committed progenitors, Lgr5<sup>-</sup>CK15<sup>+</sup> cells, which were not decreased in GVHD (Figure 2B-C). The kinetic study of the fate of Lgr5<sup>+</sup> HFSCs showed that numbers of Lgr5<sup>+</sup> HFSCs decreased both in syngeneic and allogeneic mice on day +7 after SCT, when donor T-cell infiltration had not been evident. Thereafter, numbers of HFSCs recovered to normal levels by day +21 after syngeneic SCT, but remained low after allogeneic SCT in association with massive infiltration of donor T cells in the skin (Figure 2D-E). These results demonstrate that TBI injures Lgr5<sup>+</sup> HFSCs and that the physiologic process of HFSC repopulation is inhibited by donor T cells in GVHD after allogeneic SCT. CK15<sup>+</sup> basal epithelial cells in RLPs were also decreased on day +7 after allogeneic SCT, as previously shown<sup>11,12</sup> (Figure 2F).

We then focused on the chronic phase of skin GVHD. SOX9 serves as a marker of HFSCs and is a master regulator for maintenance of HFSCs and hair-cycle progression into the growing phase, called "anagen,"<sup>22,23</sup> whereas Ki-67 is a marker of proliferating cells. Five weeks after syngeneic SCT, hair follicles elongated and reached a subcutaneous fat layer with strong expression of both SOX9 (Figure 2G) and Ki-67 (Figure 2H), indicating that hair follicles were at the anagen phase. In contrast, hair follicles in allogeneic mice remained at the resting phase, called "telogen," with only a few SOX9<sup>+</sup> and Ki-67<sup>+</sup> cells, indicating hair-cycle arrest during GVHD. Allogeneic mice developed hair follicle loss and alopecia (Figure 2I-J).

In addition to the critical role in folliculogenesis and hair regeneration during homeostasis, Lgr5<sup>+</sup> HFSCs have the capacity to reproduce all epithelial lineages and contribute to tissue regeneration after injury.<sup>5,24,25</sup> We then tested whether HFSC loss could be associated with impairment of wound healing after SCT. To confirm the contribution of HFSCs to wound healing, Lgr5 fate-mapping B6-Lgr5<sup>EGFP-cre/ER</sup>  $\times$  R26<sup>tdTomato</sup> mice, in which Lgr5<sup>+</sup> cells and their progenies were labeled with tdTomato, were wounded with a 5-mm disposable punch-biopsy instrument. Immunofluorescent study of the skin samples 10 days after wounding showed significant emergence of tdTomato<sup>+</sup> keratinocytes derived from Lgr5<sup>+</sup> HFSCs in the regenerating epithelium, but not in the intact skin of the same mice (supplemental Figure 1A-B). Wounding experiments were then performed in recipient mice 14 days after SCT. Significant numbers of

**Figure 2. GVHD reduces tissue stem cells in the skin and lingual epithelium and impairs hair and skin regeneration.** Lethally irradiated B6 or B6-Lgr5<sup>EGFP-cre/ER</sup> mice were transplanted as in Figure 1. Back skins from B6-Lgr5<sup>EGFP-cre/ER</sup> recipients were harvested on day +14 after SCT. (A) Representative immunofluorescent images of EGFP (green), CK15 (red), and DAPI (blue). Original magnification  $\times$ 40. Scale bar, 25  $\mu$ m. Numbers of Lgr5<sup>+</sup>CK15<sup>+</sup> (B) and Lgr5<sup>-</sup>CK15<sup>+</sup> (C) cells per hair follicle from 2 independent experiments (n = 6-8 per group). (D) The numbers of Lgr5<sup>+</sup> HFSCs (n = 5-6 per group) and (E) infiltrating T cells in the back skin (n = 4-6 per group) on day +7, +14, +21 after SCT from 2 independent experiments. (F) Immunofluorescent staining of CK15 (red) and DAPI (blue) in lingual sections on day +7. Original magnification  $\times$ 20. Scale bar, 50  $\mu$ m. (G-H) Representative images of immunofluorescent staining with anti-SOX9 (G) or anti-Ki-67 (H) mAbs (red) with DAPI (blue) in the skin samples harvested on day +35 after SCT. Original magnification  $\times$ 10. Scale bar, 100  $\mu$ m. (I-J) Numbers of hair follicles from independent 2 experiments (I, n = 8-9 per group) and macroscopic images of recipient mice (J) on day +35 after SCT. (K-M) Full-thickness round skin was removed from the shaved back of B6-Lgr5<sup>EGFP-cre/ER</sup>  $\times$  R26<sup>tdTomato</sup> mice after Cre recombination with tamoxifen treatment after SCT. (K) Representative immunofluorescent images of tdTomato (red), and DAPI (blue) 12 days after incision. The regenerated epithelium was marked with double-headed arrows and dot lines show epidermal-dermal junction. Original magnification  $\times$ 20. Scale bar, 50  $\mu$ m. Macroscopic images (L) and relative wound area (M) from 2 independent experiments were combined (n = 6 per group). The Mann-Whitney U test or 1-way ANOVA followed by the Tukey posttest was used to compare the data (\*\*P < .01; \*\*\*P < .005). Data represent the mean  $\pm$  SEM. dpw, days postwounding.

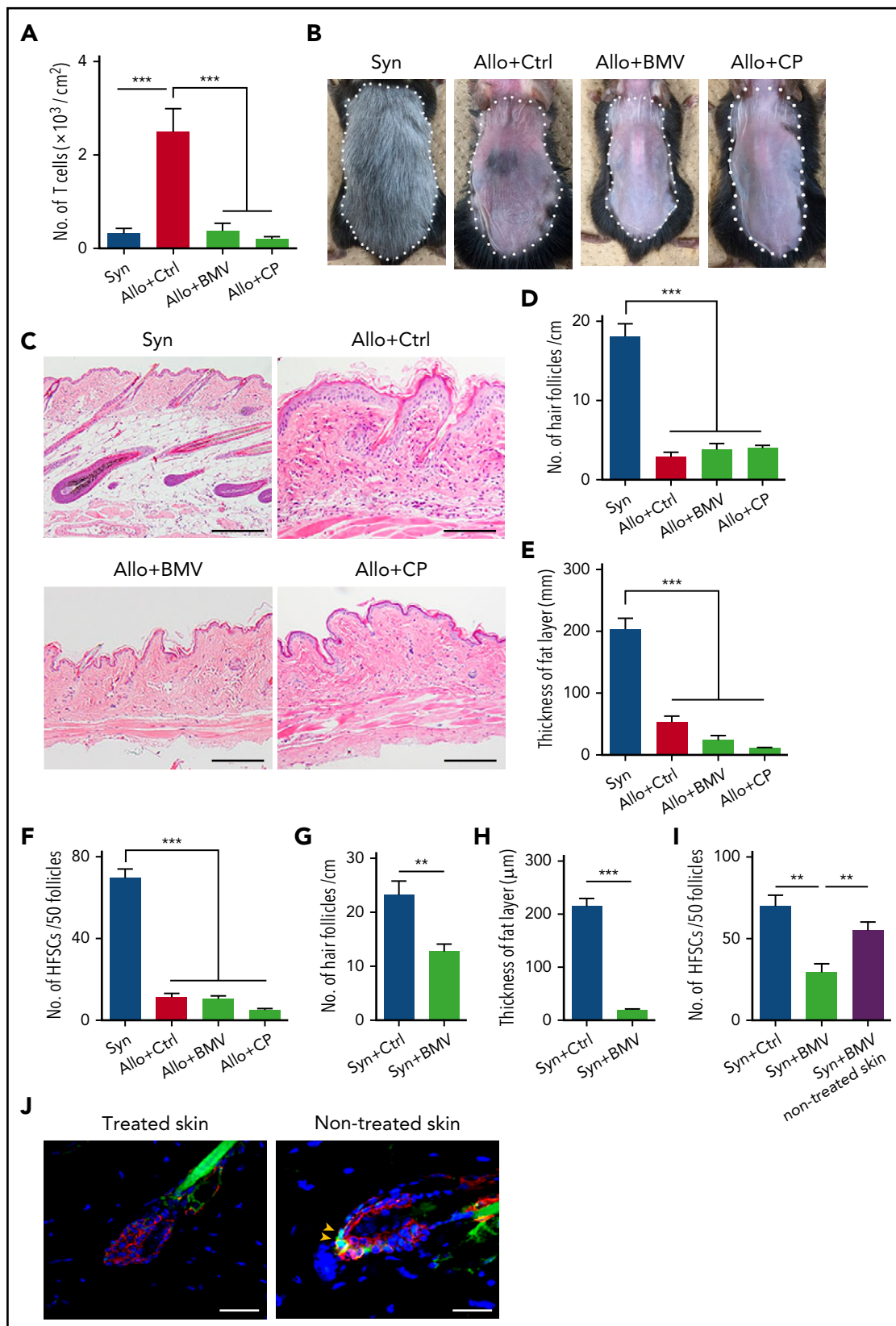


**Figure 3. Topical corticosteroids damage  $Lgr5^+$  HFSCs and induce loss of hair follicles and fat-layer atrophy in the skin.** (A–J) Lethally irradiated B6 or B6- $Lgr5^{EGFP-cre/ER}$  mice were transplanted as in Figure 1, followed by daily administration of control Vaseline (Ctrl), betamethasone valerate ointment 0.12% (BMV), or clobetasol propionate ointment 0.05% (CP) on their shaved back skin from day +1 after SCT. (A) Numbers of infiltrating donor T cells on day +14 after SCT from 2 independent experiments ( $n = 8$  per group). Representative macroscopic images (B), H&E staining of the skin sections (C), numbers of hair follicles (D), and thickness of fat layer (E) in treated skin on day +50 after SCT. Data from 2 independent experiments were combined ( $n = 6-7$  per group). The area surrounded by a dashed line shows treated skin with each ointment. Original magnification  $\times 10$ .

tdTomato<sup>+</sup> keratinocytes emerged in the regenerated skin of syngeneic mice, whereas only a few tdTomato<sup>+</sup> keratinocytes were observed in allogeneic mice (Figure 2K). When the tempo of wound healing after SCT was assessed by measuring the wound areas, wound healing was significantly delayed in allogeneic mice (Figure 2L-M). Altogether, we concluded that Lgr5<sup>+</sup> HFSCs were quantitatively and functionally damaged in skin GVHD.

### Topical corticosteroids fail to protect Lgr5<sup>+</sup> HFSCs against skin GVHD

Topical corticosteroids are broadly used to treat skin GVHD. We evaluated effects of corticosteroid ointments on skin GVHD. Betamethasone or clobetasol were administered onto shaved back skin at the clinically used concentrations, 0.12% and 0.05%, respectively, once daily after allogeneic SCT. They suppressed donor T-cell infiltration in the skin (Figure 3A) but failed to restore hair regeneration (Figure 3B) and chronic GVHD pathology, such as hair follicle loss and fat atrophy (Figure 3C-E). Furthermore, topical corticosteroids failed to mitigate Lgr5<sup>+</sup> HFSC loss in GVHD (Figure 3F). We hypothesized that the discordant effects of corticosteroids on donor T cells and skin pathology could be due to their adverse effects on the skin. To test this hypothesis, betamethasone ointment was administered after syngeneic SCT for 3 weeks. It caused significant loss of hair follicles and fat-layer atrophy (Figure 3G-H). Numbers of Lgr5<sup>+</sup> stem cells were significantly reduced only in the treated skin, but not in untreated skin of the same mice, suggesting direct toxicity of topical corticosteroids to Lgr5<sup>+</sup> HFSCs (Figure 3I-J).

### Topical ruxolitinib suppresses donor T-cell infiltration, protects HFSCs, and ameliorates skin GVHD after allogeneic SCT

Given the potential adverse effects of topical corticosteroids, we explored a novel topical therapy to protect HFSCs in GVHD. In this study, we demonstrated elevation of serum levels of IFN- $\gamma$  and upregulation of CXCR3 and its ligands in skin GVHD, as previously reported<sup>21,26</sup> (Figure 1C,L-M). IFN- $\gamma$  plays an important role in accumulation of CXCR3<sup>+</sup> T cells in inflamed tissue<sup>27,28</sup> and thereby disrupts the immune privilege of hair bulge in lichen planopilaris, localized scalp hair loss.<sup>29</sup> We hypothesized that inhibition of IFN- $\gamma$  receptor signaling by topical administration of JAK1/2 inhibitor ruxolitinib could prevent donor T-cell infiltration in the skin and protect HFSCs from IFN- $\gamma$ -induced immune privilege collapse of hair bulge. Topical administration of ruxolitinib ointment prevented CXCL9 upregulation in the skin of naive mice administered with IFN- $\gamma$ , confirming efficacy of this ointment (supplemental Figure 2). When administered onto the shaved back skin of recipient mice once daily after SCT, ruxolitinib significantly suppressed skin infiltration of donor T cells, including IFN- $\gamma$ -producing T cells and IL-17A-producing T cells and their progenies, which play an important role for the pathogenesis of skin GVHD<sup>30</sup> (Figure 4A-C), without inducing any skin side effects, such as bruises or infectious lesions,

detected by visual inspection and histological examination of the skin. Ruxolitinib suppressed skin infiltration of CXCR3-expressing donor T cells (Figure 4D) and skin expression of CXCR3 ligands, *Cxcl9*, *Cxcl10*, and *Cxcl11* on day +14 after SCT (Figure 4E). Ruxolitinib subsequently ameliorated GVHD pathology and suppressed the fat-layer atrophy on day +28 after SCT (Figure 4F). In sharp contrast to topical corticosteroids, ruxolitinib protected Lgr5<sup>+</sup> HFSCs against GVHD and induced hair regeneration (Figure 4G-I).

Posttransplant wound healing tested on day +21 after SCT was significantly improved in ruxolitinib-treated mice to the levels of syngeneic controls, whereas betamethasone failed to facilitate wound healing (Figure 4J). When mice were wounded on day +28, topical ruxolitinib again significantly facilitated wound healing (supplemental Figure 3). We tested whether topical ruxolitinib could attenuate the toxicity of topical corticosteroids when given concurrently with corticosteroids from day +1 after syngeneic SCT. The number of HFSCs and thickness of fat layer were comparable between mice treated with betamethasone alone and those with betamethasone plus ruxolitinib, indicating that topical ruxolitinib failed to mitigate the steroid-induced toxicities on skin homeostasis (supplemental Figure 4A-B).

We next evaluated impact of discontinuation of topical ruxolitinib on skin GVHD. Discontinuation of ruxolitinib on day +15 resulted in significant exaggeration of pathological cutaneous GVHD and prompt loss of Lgr5<sup>+</sup> HFSCs in a week (Figure 4K-M), and also exacerbated pathology of chronic GVHD such as dermal fibrosis at a later time point (Figure 4N-O). These results indicate that discontinuation of topical ruxolitinib results in GVHD exaggeration in the absence of systemic immunosuppressive treatment.

We also confirmed that systemic administration of ruxolitinib protected HFSCs against GVHD (supplemental Figure 5A). However, there were no synergistic protective effects of systemic and topical administration of ruxolitinib. Again, systemic steroids did not protect HFSCs despite significant suppression of donor T-cell infiltration in the skin after allogeneic SCT (supplemental Figure 5A-B). As previously reported,<sup>31</sup> systemic administration of ruxolitinib significantly decreased serum levels of tumor necrosis factor  $\alpha$ , increased the number of regulatory T cells, and ameliorated systemic GVHD scores after allogeneic SCT (supplemental Figure 6A-C). On the other hand, topical ruxolitinib had no effects on donor T-cell expansion in the spleens, immune reconstitution as assessed by the numbers of CD4<sup>+</sup>CD8<sup>+</sup> double-positive cells in the thymus, systemic clinical GVHD scores, and pathological GVHD scores in the untreated skin, liver, and gut (supplemental Figure 7A-D). These data indicate that topical ruxolitinib ameliorates skin GVHD without affecting systemic immunity. Ruxolitinib also protected CK15<sup>+</sup> epidermal stem cells in the tongue, suggesting that ruxolitinib could protect

**Figure 3 (continued)** Scale bar, 100  $\mu$ m. (F) EGFP<sup>+</sup> cells in 50 follicles of treated skin on day +14 after SCT from 2 independent experiments (n = 6-7 per group). (G-J) Lethally irradiated B6 or B6-Lgr5<sup>EGFP-cre/ER</sup> mice were transplanted with 5  $\times$  10<sup>6</sup> bone marrow cells and 5  $\times$  10<sup>6</sup> splenocytes from syngeneic B6 mice and administered daily with each ointment onto back skin for 3 weeks after SCT. Numbers of hair follicles (G) (n = 10 per group), thickness of fat layer (H) (n = 10 per group), and numbers of EGFP<sup>+</sup> cells in 50 follicles (I) (n = 7 per group) from 2 independent experiments were combined. (J) Representative immunofluorescent images of EGFP (green), CK15 (red), and DAPI (blue) of the treated skin and nontreated skin of the syngeneic animal. Original magnification  $\times$ 40. Scale bar, 50  $\mu$ m. One-way ANOVA followed by the Tukey posttest was used to compare the data (\*\*P < .005; \*\*P < .01). Data represent the mean  $\pm$  SEM.

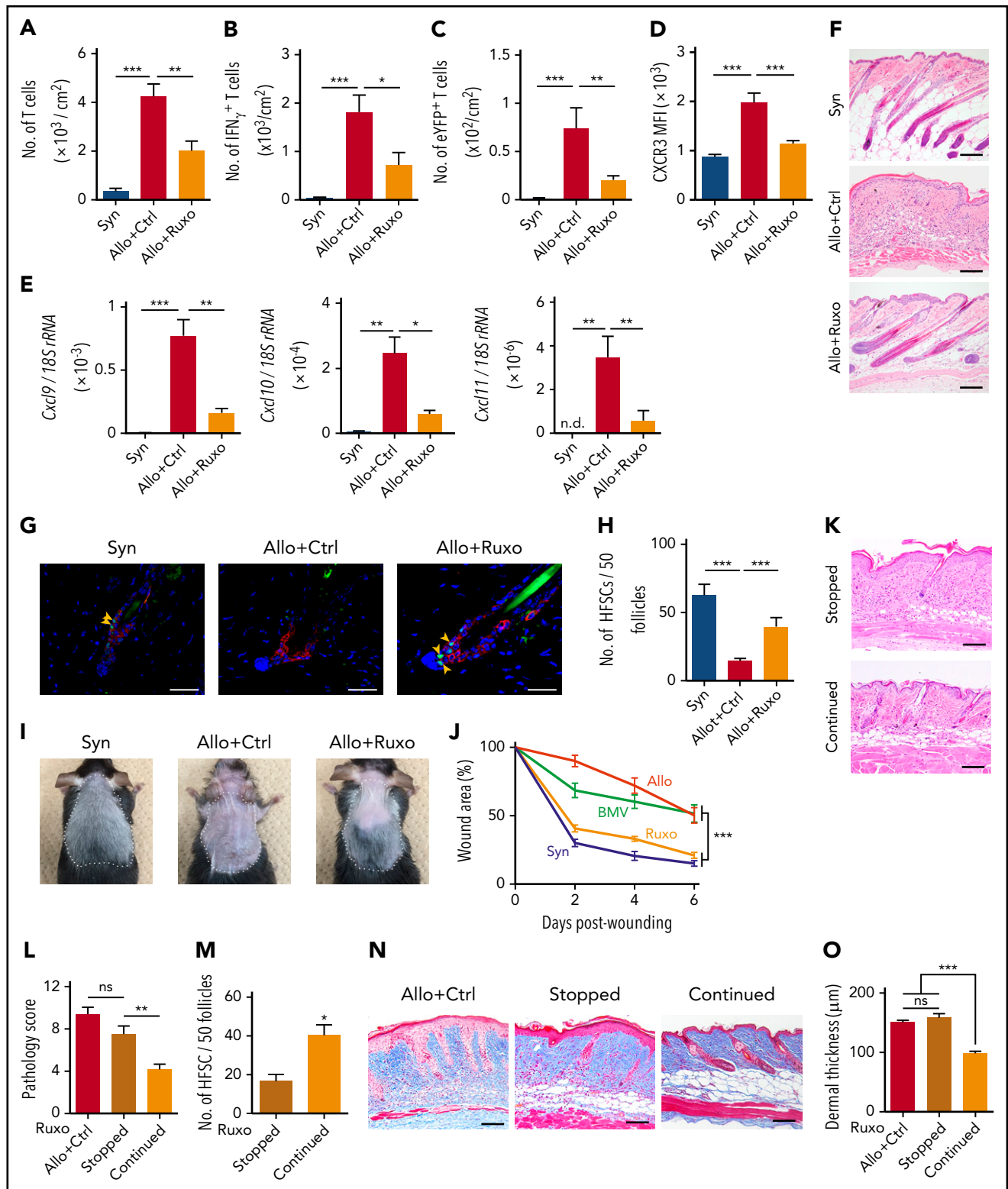


**Figure 4. Topical ruxolitinib ameliorates skin GVHD, protects  $\text{Lgr5}^+$  HFSCs against skin GVHD, and promotes hair regeneration and wound healing.** B6 or B6- $\text{Lgr5}^{\text{EGFP-cre/ER}}$  mice were transplanted as in Figure 1. (A-J) Recipients were treated daily with Vaseline (Ctrl) or ruxolitinib (Ruxo) ointment on their shaved back skin from day +1 after SCT. (A-E) Numbers of T cells (A),  $\text{IFN}_\gamma$  T cells (B), IL-17-eYFP+ T cells (C) and MFI of CXCR3 on T cells (D), and expression levels of *Cxcl9*, *Cxcl10*, and *Cxcl11* (E) measured by Q-PCR on day +14. Data from 3 independent experiments ( $n = 6-10$  per group). (F) H&E staining of skin samples on day +28 after SCT. Original magnification  $\times 10$ . Scale bar, 100  $\mu\text{m}$ . (G) Immunofluorescent staining of the skin samples on day +14 after SCT with EGFP (green), CK15 (red), and DAPI (blue). Original magnification  $\times 40$ . Scale bar, 50  $\mu\text{m}$ . (H) Numbers of EGFP+ cells per 50 follicles from 2 independent experiments ( $n = 6-7$  per group). (I) Macroscopic images of hair regeneration in the treated skin on day +35 after SCT. The treated areas are surrounded by dashed lines. (J) Mice were treated with each ointment from day +1 to day +21 after SCT. Full-thickness wounds were made on the back skin of recipient mice on day +21. Wound areas of syngeneic (Syn; blue), allogeneic control (Allo; red), allogeneic plus BMV (green), and allogeneic plus ruxolitinib (Ruxo; orange) from 2 independent experiments. (K-O) Ruxolitinib ointment was stopped on day +15 (Stopped) or continued thereafter (Continued). The representative images of H&E staining (K; scale bar, 100  $\mu\text{m}$ ), pathology skin GVHD



other tissue stem cells than Lgr5<sup>+</sup> HFSCs against GVHD (supplemental Figure 8).

### Topical ruxolitinib improves established skin GVHD and protects Lgr5<sup>+</sup> HFSCs

Given the therapeutic effects of systemic ruxolitinib on established systemic acute GVHD (supplemental Figure 9A-B), we finally evaluated efficacy of topical ruxolitinib to treat established skin GVHD. Ruxolitinib ointment was administered onto the shaved back skin from day +10 after SCT, when acute skin GVHD with significant donor T-cell infiltration had already been observed (Figure 1G). Analysis of the skin samples harvested on day +21 after SCT showed that topical ruxolitinib suppressed T-cell expansion in the treated skin, improved pathological scores, and protected Lgr5<sup>+</sup> HFSCs against GVHD (Figure 5A-C). T-cell proliferation assessed by Ki-67 staining of donor T cells was significantly suppressed after 5-day treatment with topical ruxolitinib, whereas apoptosis assessed by Annexin V staining was not changed by ruxolitinib. These data suggest that topical ruxolitinib ameliorated established skin GVHD by suppressing local proliferation of donor T cells without inducing T-cell apoptosis (Figure 5D-G).

## Discussion

Emerging data indicate that GVHD causes damage to ISCs.<sup>1,2</sup> In the skin, various types of stem cells or progenitor cells in hair follicle and interfollicular epithelium maintain homeostasis of distinct compartments of the skin in steady state.<sup>5,7,8,24,25</sup> The best-characterized stem cell population in the skin is HFSCs; HFSCs with lineage plasticity and the multipotent capacity to reproduce epidermis in repair are Lgr5<sup>+</sup>.<sup>5,8,24,25</sup> Previous studies showed that apoptosis and donor T-cell infiltration were spatially restricted to the sites harboring stem cell populations such as bulge regions of hair follicles and human epidermal rete ridges.<sup>9-15</sup> In this study, we affirm the long-held assumption that HFSCs may be targets for GVHD.<sup>10</sup>

Loss of stem cells was functionally associated with delayed wound repair and alopecia that were independent of conditioning regimen. Although it is well appreciated that chemotherapy and irradiation damage hair follicles and induce alopecia, hair loss is also one of the distinguished features of clinical chronic GVHD.<sup>32,33</sup> The hair follicles undergo a cyclical regression and regeneration process consisting of 3 phases: anagen, catagen, and telogen.<sup>34</sup> Because proliferation of HFSCs is essential for hair follicles to enter the anagen phase,<sup>35</sup> it seems that loss of HFSCs is associated with hair-cycle arrest in the telogen phase in GVHD. We observed delayed wound healing in GVHD in this study. Poor wound healing is also a clinical manifestation of skin GVHD.<sup>32</sup> HFSCs play a significant role in wound healing; in the early phase of wound healing, they give rise to keratinocytes that contribute to wound re-epithelialization.<sup>24,36</sup> The tempo of wound healing is significantly delayed in the hairless skin, where HFSCs are lacking, compared with the haired skin.<sup>37</sup>

Target cell injury in GVHD is mediated by both effector functions of donor cytotoxic T cells and inflammatory cytokines. Cytotoxic T cells induce epidermal injury in GVHD and satellitosis showing that lymphocytes surrounding an apoptotic target cell are a hallmark of skin GVHD pathology. Thus, it is highly likely that donor T cells directly kill HFSCs. On the other hand, inflammatory cytokines secreted from donor T cells may directly induce apoptosis of HFSCs as previously shown in CK15<sup>+</sup> epidermal stem cells in the RLPs.<sup>11,38</sup> Further comprehensive studies are required to address effector mechanisms of skin stem cell injury.

Interestingly, Lgr5<sup>+</sup>CK15<sup>+</sup> HFSCs were more susceptible to GVHD than Lgr5<sup>-</sup>CK15<sup>+</sup> progenitors. Differential cell-cycle status or differential susceptibility to cytotoxic effectors between stem cells and differentiated cells may be associated with this phenomenon. A previous study showed that proinflammatory cytokines preferentially induce expression of proapoptotic molecules in CK15<sup>+</sup> stem cells in RLPs during GVHD, resulting in selective apoptosis of these cell population, while sparing mature epithelium.<sup>38</sup> Recently, it was proposed that the difference of "tissue tolerance," the tissue-specific capacity to maintain parenchymal-tissue homeostasis during inflammation could be associated with differential susceptibility of tissues to diseases.<sup>39</sup> High sensitivity of the skin and ISCs to inflammatory milieu during GVHD may explain the high incidence of skin and gut involvement in acute GVHD.

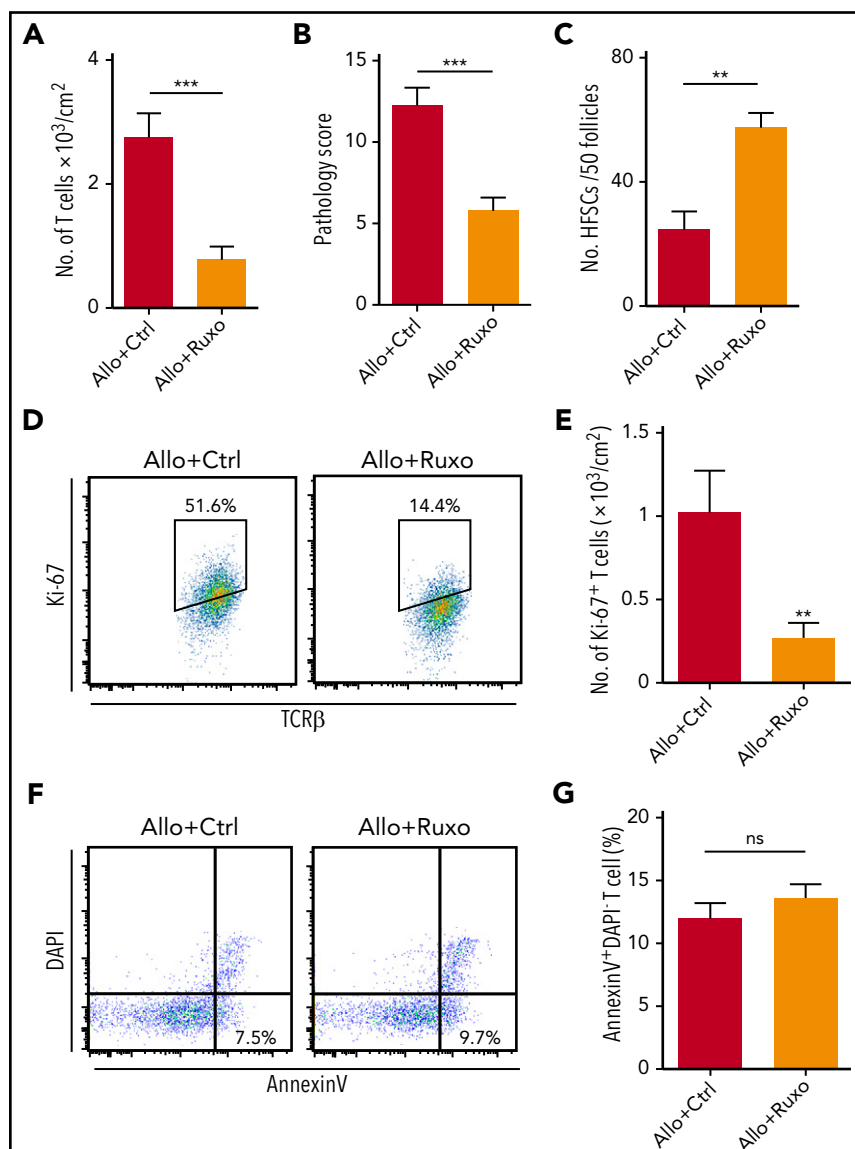
The bulge region in the hair follicles is a site of relative immune privilege with less antigen presentation and expression of immunosuppressive molecules in immunological conditions such as skin allograft.<sup>40,41</sup> It is possible that the inflammatory milieu after allogeneic SCT may break immune privilege of hair follicles. Interestingly, stress-induced chemokine upregulation in the hair follicles recruits the precursor of Langerhans cells, the major antigen-presenting cells in skin GVHD, into the hair follicles.<sup>42-44</sup> Similarly, we and others recently showed that alloreactive donor T cells could infiltrate to immune-privilege tissues, such as the ovary and testis, in the inflammatory milieu in GVHD.<sup>45,46</sup>

Current standard therapy for a variety of skin diseases is topical administration of corticosteroids.<sup>47,48</sup> However, pathogenic T cells often resist corticosteroid-induced apoptosis,<sup>49</sup> and long-term use of topical corticosteroids induces adverse effects on the skin such as skin atrophy and delayed wound healing by inhibiting keratinocyte proliferation.<sup>16,50</sup> Our study further demonstrates that topical corticosteroids induce loss of Lgr5<sup>+</sup> HFSCs and such HFSC damage may be a potential mechanism of adverse effects of corticosteroids on the skin.

JAK1/2 relays multiple cytokine signals and plays an important role in activation and migration of antigen-specific T cells.<sup>51,52</sup> It has been demonstrated that systemic administration of JAK1/2 inhibitor ruxolitinib is effective in treatment of steroid-refractory acute and chronic GVHD.<sup>53,54</sup> Topical ruxolitinib may have significant advantages that help avoid frequent complications of

**Figure 4 (continued)** scores (L) and the numbers of Lgr5<sup>+</sup> HFSCs in the treated skin (M) on day +21 after allogeneic SCT from 2 independent experiments (n = 5-6 per group) were shown. Representative images of Masson trichrome staining (N; scale bar, 100 μm) and dermal thickness of treated skin (O; n = 6-7 per group) on day +35 from 2 independent experiments. The Mann-Whitney U test or 1-way ANOVA followed by Tukey posttest was used to compare the data (\*P < .05; \*\*P < .01; \*\*\*P < .005). Data represent the mean ± SEM.

**Figure 5. Therapeutic administration of topical ruxolitinib ameliorates established skin GVHD and protects HFSCs.** (A-G) Lethally irradiated B6 mice were transplanted as in Figure 1. Recipient mice were treated with ruxolitinib ointment from day +10 after allogeneic SCT. Number of donor T cells (A), pathological skin GVHD scores (B) ( $n = 7-9$  per group), and numbers of EGFP<sup>+</sup> cells in 50 follicles on day +21 (C;  $n = 6$  per group). (D-G) Ki-67 staining (D-E) and Annexin V assay (F-G) of donor T cells from the treated skin were performed on day +15 after allogeneic SCT ( $n = 8-9$  per group). Data from 2 independent experiments were combined and shown as the mean  $\pm$  SEM. The Mann-Whitney *U* test was used to compare the data (\* $P < .05$ ; \*\* $P < .01$ ; \*\*\* $P < .005$ ). ns, not significant; TCR, T-cell receptor.



systemic ruxolitinib use such as cytopenias and opportunistic infections. We found that topical ruxolitinib ameliorated skin GVHD by suppressing infiltration of donor Th1 and Th17 cells equivalently to topical corticosteroid, as demonstrated in studies of systemic administration of ruxolitinib.<sup>31,51,55</sup> Recent studies demonstrated that topical ruxolitinib attenuated IFN- $\gamma$  signaling, inhibited T-cell infiltration in the skin, and ameliorated experimental alopecia areata.<sup>56,57</sup> Topical ruxolitinib is now being investigated in clinical trials for alopecia areata and psoriasis.<sup>58</sup> A recent study demonstrated that ruxolitinib promoted hair growth by activating mesenchymal cells in dermal papilla.<sup>59</sup> Our study further demonstrates that in sharp contrast to corticosteroids, topical ruxolitinib protects Lgr5<sup>+</sup> HFSCs and their putative niche, fat tissue,<sup>60,61</sup> thereby maintaining skin homeostasis and regeneration, suggesting that topical ruxolitinib has significant advantage over topical corticosteroids for treatment of inflammatory skin diseases.

In summary, our study demonstrates a novel mechanism of skin injury in GVHD and proposes potentially superior therapeutic

strategy over corticosteroids, the long-term standard of care for a variety of skin diseases. Topical administration of JAK inhibitors is a promising therapeutic strategy for skin GVHD and other autoimmune diseases in the skin without adverse effects on the skin and skin stem cells.

## Acknowledgments

This work was supported by Japan Society for the Promotion of Science KAKENHI (17H04206 and 25293217 [T.T.], 17K09945 and 26461438 [D.H.]), the Center of Innovation Program from the Japan Science and Technology Agency (T.T.), Promotion and Standardization of the Tenure-Track System (D.H.), and the Suhara Foundation (D.H.).

## Authorship

Contribution: D.H. and T.T. developed the conceptual framework of the study, designed the experiments, conducted experiments, analyzed data, and wrote the paper; S.T. conducted experiments, analyzed data, and wrote the paper; E.H., R.O., H.O., T.A., E.Y., K.E., and S.M. conducted experiments; and G.R.H., J.S., and M.O. supervised experiments.

Conflict-of-interest disclosure: T.T. is a consultant of Novartis Pharma. The remaining authors declare no competing financial interests.

ORCID profiles: S.T., 0000-0002-3850-0559; D.H., 0000-0001-9489-9704; T.T., 0000-0002-0941-271X.

Correspondence: Takanori Teshima, Department of Hematology, Graduate School of Medicine, Faculty of Medicine, Hokkaido University, N15 W7, Kita-ku, Sapporo 060-8638, Japan; e-mail: teshima@med.hokudai.ac.jp; and Daigo Hashimoto, Department of Hematology, Graduate School of Medicine, Faculty of Medicine, Hokkaido University, N15 W7, Kita-ku, Sapporo 060-8638, Japan; e-mail: d5hash@pop.med.hokudai.ac.jp.

## REFERENCES

1. Takashima S, Kadowaki M, Aoyama K, et al. The Wnt agonist R-spondin1 regulates systemic graft-versus-host disease by protecting intestinal stem cells. *J Exp Med*. 2011;208(2):285-294.
2. Hanash AM, Dudakov JA, Hua G, et al. Interleukin-22 protects intestinal stem cells from immune-mediated tissue damage and regulates sensitivity to graft versus host disease. *Immunity*. 2012;37(2):339-350.
3. Lindemans CA, Calafiore M, Mertelsmann AM, et al. Interleukin-22 promotes intestinal-stem-cell-mediated epithelial regeneration. *Nature*. 2015;528(7583):560-564.
4. Ratanatharathorn V, Nash RA, Przepiora D, et al. Phase III study comparing methotrexate and tacrolimus (prograf, FK506) with methotrexate and cyclosporine for graft-versus-host disease prophylaxis after HLA-identical sibling bone marrow transplantation. *Blood*. 1998;92(7):2303-2314.
5. Page ME, Lombard P, Ng F, Göttgens B, Jensen KB. The epidermis comprises autonomous compartments maintained by distinct stem cell populations. *Cell Stem Cell*. 2013;13(4):471-482.
6. Liu Y, Lyle S, Yang Z, Cotsarelis G. Keratin 15 promoter targets putative epithelial stem cells in the hair follicle bulge. *J Invest Dermatol*. 2003;121(5):963-968.
7. Schepeler T, Page ME, Jensen KB. Heterogeneity and plasticity of epidermal stem cells. *Development*. 2014;141(13):2559-2567.
8. Jaks V, Barker N, Kasper M, et al. Lgr5 marks cycling, yet long-lived, hair follicle stem cells. *Nat Genet*. 2008;40(11):1291-1299.
9. Sale GE, Shulman HM, Gallucci BB, Thomas ED. Young rete ridge keratinocytes are preferred targets in cutaneous graft-versus-host disease. *Am J Pathol*. 1985;118(2):278-287.
10. Sale GE, Beauchamp MD, Akiyama M. Para-follicular bulges, but not hair bulb keratinocytes, are attacked in graft-versus-host disease of human skin. *Bone Marrow Transplant*. 1994;14(3):411-413.
11. Whitaker-Menezes D, Jones SC, Friedman TM, Korngold R, Murphy GF. An epithelial target site in experimental graft-versus-host disease and cytokine-mediated cytotoxicity is defined by cytokeratin 15 expression. *Biol Blood Marrow Transplant*. 2003;9(9):559-570.
12. Zhan Q, Signoretti S, Whitaker-Menezes D, Friedman TM, Korngold R, Murphy GF. Cytokeratin15-positive basal epithelial cells targeted in graft-versus-host disease express a constitutive antiapoptotic phenotype. *J Invest Dermatol*. 2007;127(1):106-115.
13. Murphy GF, Lavker RM, Whitaker D, Korngold R. Cytotoxic folliculitis in GvHD. Evidence of follicular stem cell injury and recovery. *J Cutan Pathol*. 1991;18(5):309-314.
14. Murphy GF, Korngold R. Significance of selectively targeted apoptotic rete cells in graft-versus-host disease. *Biol Blood Marrow Transplant*. 2004;10(6):357-365.
15. Gilliam AC, Whitaker-Menezes D, Korngold R, Murphy GF. Apoptosis is the predominant form of epithelial target cell injury in acute experimental graft-versus-host disease. *J Invest Dermatol*. 1996;107(3):377-383.
16. Abraham A, Roga G. Topical steroid-damaged skin. *Indian J Dermatol*. 2014;59(5):456-459.
17. Hill GR, Olver SD, Kuns RD, et al. Stem cell mobilization with G-CSF induces type 17 differentiation and promotes scleroderma. *Blood*. 2010;116(5):819-828.
18. Cooke KR, Kobzik L, Martin TR, et al. An experimental model of idiopathic pneumonia syndrome after bone marrow transplantation: I. The roles of minor H antigens and endotoxin. *Blood*. 1996;88(8):3230-3239.
19. Hirota K, Duarte JH, Veldhoen M, et al. Fate mapping of IL-17-producing T cells in inflammatory responses. *Nat Immunol*. 2011;12(3):255-263.
20. Uryu H, Hashimoto D, Kato K, et al.  $\alpha$ -Mannan induces Th17-mediated pulmonary graft-versus-host disease in mice. *Blood*. 2015;125(19):3014-3023.
21. He S, Cao Q, Qiu Y, et al. A new approach to the blocking of alloreactive T cell-mediated graft-versus-host disease by in vivo administration of anti-CXCR3 neutralizing antibody. *J Immunol*. 2008;181(11):7581-7592.
22. Adam RC, Yang H, Rockowitz S, et al. Pioneer factors govern super-enhancer dynamics in stem cell plasticity and lineage choice. *Nature*. 2015;521(7552):366-370.
23. Nowak JA, Polak L, Pasolli HA, Fuchs E. Hair follicle stem cells are specified and function in early skin morphogenesis. *Cell Stem Cell*. 2008;3(1):33-43.
24. Ito M, Liu Y, Yang Z, et al. Stem cells in the hair follicle bulge contribute to wound repair but not to homeostasis of the epidermis. *Nat Med*. 2005;11(12):1351-1354.
25. Levy V, Lindon C, Zheng Y, Harfe BD, Morgan BA. Epidermal stem cells arise from the hair follicle after wounding. *FASEB J*. 2007;21(7):1358-1366.
26. Piper KP, Horlock C, Curnow SJ, et al. CXCL10-CXCR3 interactions play an important role in the pathogenesis of acute graft-versus-host disease in the skin following allogeneic stem-cell transplantation. *Blood*. 2007;110(12):3827-3832.
27. Groom JR, Luster AD. CXCR3 ligands: redundant, collaborative and antagonistic functions. *Immunol Cell Biol*. 2011;89(2):207-215.
28. Choi J, Ziga ED, Ritchey J, et al. IFN $\gamma$ R signaling mediates alloreactive T-cell trafficking and GVHD. *Blood*. 2012;120(19):4093-4103.
29. Harries MJ, Meyer K, Chaudhry I, et al. Lichen planopilaris is characterized by immune privilege collapse of the hair follicle's epithelial stem cell niche. *J Pathol*. 2013;231(2):236-247.
30. Gartlan KH, Markey KA, Varelias A, et al. Tc17 cells are a proinflammatory, plastic lineage of pathogenic CD8+ T cells that induce GVHD without antileukemic effects. *Blood*. 2015;126(13):1609-1620.
31. Spoerl S, Mathew NR, Bscheider M, et al. Activity of therapeutic JAK 1/2 blockade in graft-versus-host disease. *Blood*. 2014;123(24):3832-3842.
32. Jagasia MH, Greinix HT, Arora M, et al. National Institutes of Health Consensus Development Project on Criteria for Clinical Trials in Chronic Graft-versus-Host Disease: I. The 2014 Diagnosis and Staging Working Group report. *Biol Blood Marrow Transplant*. 2015;21(3):389-401.
33. Basilio FM, Brenner FM, Werner B, Rastelli GJ. Clinical and histological study of permanent alopecia after bone marrow transplantation. *An Bras Dermatol*. 2015;90(6):814-821.
34. Alonso L, Fuchs E. The hair cycle. *J Cell Sci*. 2006;119(Pt 3):391-393.
35. Morris RJ, Liu Y, Marles L, et al. Capturing and profiling adult hair follicle stem cells. *Nat Biotechnol*. 2004;22(4):411-417.
36. Mascré G, Dekoninck S, Drogat B, et al. Distinct contribution of stem and progenitor cells to epidermal maintenance. *Nature*. 2012;489(7415):257-262.
37. Langton AK, Herrick SE, Headon DJ. An extended epidermal response heals cutaneous wounds in the absence of a hair follicle stem cell contribution. *J Invest Dermatol*. 2008;128(5):1311-1318.

## Footnotes

Submitted 22 June 2017; accepted 21 January 2018. Prepublished online as *Blood* First Edition paper, 23 January 2018; DOI 10.1182/blood-2017-06-792614.

The online version of this article contains a data supplement.

The publication costs of this article were defrayed in part by page charge payment. Therefore, and solely to indicate this fact, this article is hereby marked "advertisement" in accordance with 18 USC section 1734.

38. Zhan Q, Korngold R, Lezcano C, McKeon F, Murphy GF. Graft-versus-host disease-related cytokine-driven apoptosis depends on p73 in cytokeratin 15-positive target cells. *Biol Blood Marrow Transplant*. 2012;18(6):841-851.
39. Wu SR, Reddy P. Tissue tolerance: a distinct concept to control acute GVHD severity. *Blood*. 2017;129(13):1747-1752.
40. Meyer KC, Klatter JE, Dinh HV, et al. Evidence that the bulge region is a site of relative immune privilege in human hair follicles. *Br J Dermatol*. 2008;159(5):1077-1085.
41. Paus R, Nickoloff BJ, Ito T. A 'hairy' privilege. *Trends Immunol*. 2005;26(1):32-40.
42. Nagao K, Kobayashi T, Moro K, et al. Stress-induced production of chemokines by hair follicles regulates the trafficking of dendritic cells in skin. *Nat Immunol*. 2012;13(8):744-752.
43. Merad M, Hoffmann P, Ranheim E, et al. Depletion of host Langerhans cells before transplantation of donor alloreactive T cells prevents skin graft-versus-host disease [published correction appears in *Nat Med*. 2004;10(6):649]. *Nat Med*. 2004;10(5):510-517.
44. Kreutz M, Karrer S, Hoffmann P, et al. Whole-body UVB irradiation during allogeneic hematopoietic cell transplantation is safe and decreases acute graft-versus-host disease. *J Invest Dermatol*. 2012;132(1):179-187.
45. Shimoji S, Hashimoto D, Tsujigiwa H, et al. Graft-versus-host disease targets ovary and causes female infertility in mice. *Blood*. 2017;129(9):1216-1225.
46. Wagner AM, Beier K, Christen E, Holländer GA, Krenger W. Leydig cell injury as a consequence of an acute graft-versus-host reaction. *Blood*. 2005;105(7):2988-2990.
47. Wolff D, Schleuning M, von Harsdorf S, et al. Consensus Conference on Clinical Practice in Chronic GVHD: Second-Line Treatment of Chronic Graft-versus-Host Disease. *Biol Blood Marrow Transplant*. 2011;17(1):1-17.
48. Dignan FL, Clark A, Amrolia P, et al; British Society for Blood and Marrow Transplantation. Diagnosis and management of acute graft-versus-host disease. *Br J Haematol*. 2012;158(1):30-45.
49. Ramesh R, Kozhaya L, McKevitt K, et al. Pro-inflammatory human Th17 cells selectively express P-glycoprotein and are refractory to glucocorticoids. *J Exp Med*. 2014;211(1):89-104.
50. Chebotayev DV, Yemelyanov AY, Lavker RM, Budunova IV. Epithelial cells in the hair follicle bulge do not contribute to epidermal regeneration after glucocorticoid-induced cutaneous atrophy. *J Invest Dermatol*. 2007;127(12):2749-2758.
51. Choi J, Cooper ML, Alahmari B, et al. Pharmacologic blockade of JAK1/JAK2 reduces GvHD and preserves the graft-versus-leukemia effect. *PLoS One*. 2014;9(10):e109799.
52. O'Shea JJ, Schwartz DM, Villarino AV, Gadina M, McInnes IB, Laurence A. The JAK-STAT pathway: impact on human disease and therapeutic intervention. *Annu Rev Med*. 2015;66(1):311-328.
53. Zeiser R, Burchert A, Lengerke C, et al. Ruxolitinib in corticosteroid-refractory graft-versus-host disease after allogeneic stem cell transplantation: a multicenter survey. *Leukemia*. 2015;29(10):2062-2068.
54. Mori Y, Ikeda K, Inomata T, et al. Ruxolitinib treatment for GvHD in patients with myelofibrosis. *Bone Marrow Transplant*. 2016;51(12):1584-1587.
55. Carniti C, Gimondi S, Vendramin A, et al. Pharmacologic inhibition of JAK1/JAK2 signaling reduces experimental murine acute GVHD while preserving GVT effects. *Clin Cancer Res*. 2015;21(16):3740-3749.
56. Xing L, Dai Z, Jabbari A, et al. Alopecia areata is driven by cytotoxic T lymphocytes and is reversed by JAK inhibition. *Nat Med*. 2014;20(9):1043-1049.
57. Adachi T, Kobayashi T, Sugihara E, et al. Hair follicle-derived IL-7 and IL-15 mediate skin-resident memory T cell homeostasis and lymphoma. *Nat Med*. 2015;21(11):1272-1279.
58. Hsu L, Armstrong AW. JAK inhibitors: treatment efficacy and safety profile in patients with psoriasis. *J Immunol Res*. 2014;2014:283617.
59. Harel S, Higgins CA, Cerise JE, et al. Pharmacologic inhibition of JAK-STAT signaling promotes hair growth. *Sci Adv*. 2015;1(9):e1500973.
60. Huang CF, Chang YJ, Hsueh YY, et al. Assembling composite dermal papilla spheres with adipose-derived stem cells to enhance hair follicle induction [published correction appears in *Sci Rep*. 2016;6:31257]. *Sci Rep*. 2016;6(1):26436.
61. Festa E, Fretz J, Berry R, et al. Adipocyte lineage cells contribute to the skin stem cell niche to drive hair cycling. *Cell*. 2011;146(5):761-771.